

Gas-Phase Reaction of Silylene with Acetone: Direct Rate Studies, RRKM Modeling, and ab Initio Studies of the Potential Energy Surface

R. Becerra

Instituto de Química Física “Rocasolano”, CSIC, C/Serrano 119, 28006 Madrid, Spain

J. P. Cannady

Dow Corning Corporation, P.O. Box 995, Mail 128, Midland, Michigan, 48686-0995

R. Walsh*

Department of Chemistry, University of Reading, Whiteknights, P.O. Box 224, Reading RG6 6AD, U.K.

Received: January 7, 1999; In Final Form: March 19, 1999

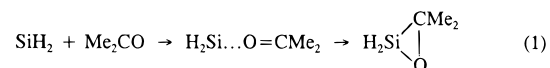
Time-resolved studies of the title reaction have been carried out over the pressure range 3–100 Torr (with SF₆ as bath gas) at five temperatures in the range 295–602 K, using laser flash photolysis to generate and monitor silylene, SiH₂. The second-order rate constants obtained were pressure-dependent, indicating that the reaction is a third-body-assisted association process. The high-pressure rate constants, obtained by extrapolation, gave the following Arrhenius parameters: $\log(A/\text{cm}^3 \text{ molecule}^{-1} \text{ s}^{-1}) = -10.17 \pm 0.04$ and $E_a = -4.54 \pm 0.32 \text{ kJ mol}^{-1}$, where the uncertainties are single standard deviations. The parameters are consistent with a fast association process occurring at close to the collision rate. RRKM modeling, based on a transition state appropriate to formation of a three-membered ring product, 3,3-dimethylsiloxirane, and employing a weak collisional deactivation model, gives reasonable fits to the pressure-dependent curves for $\Delta H^\circ/\text{kJ mol}^{-1}$ in the range –205 to –225. Ab initio calculations at the G2 level indicate the initial formation of a silacarbonyl ylid, which can then either form the siloxirane by ring closure or rearrange to form 2-siloxyprene. Fuller details of the potential surface are given. The energetics are consistent with siloxirane formation representing the main pathway.

Introduction

Silylenes are widely recognized as important intermediates in silicon hydride and organosilicon chemistry. They exist as ground-state singlets, and their characteristic reactions include insertions into Si–H, Si–OR, and O–H bonds and π -type additions across C=C and C≡C bonds.^{1,2} While early mechanistic information (pre-1985) came largely from end-product analytical studies, in recent years it has been based on an increasing number of direct, time-resolved kinetic studies of silylene reactions, which are providing a steadily accumulating database of absolute rate constants.^{3–5} Alongside experiment, theoretical studies have played an increasing role in elucidating mechanisms.^{6,7}

Studies in our own laboratories of the kinetics of reactions of SiH₂ with alkenes^{8–10} and alkynes^{11,12} have shown them to be pressure-dependent association processes occurring at close to the collision rate (at their high-pressure limits). Rice, Ramsperger, Kassel, Marcus (RRKM) theoretical modeling studies of these pressure dependencies have shown them to be consistent with the formation of silirane and silirene rings, and the experimental results have yielded information about the strain energies of these rings. Isotopic labeling studies^{4,5,12,13} have revealed the presence of scrambling mechanisms consistent with facile and reversible ring-opening reactions of siliranes and silirenes, leading to formation of isomeric alkyl- and alkenyl-silylenes, as suggested by earlier product analytical studies^{14–19} and supported by theoretical calculations.^{20–23}

As part of a series of studies focused on reactions with the potential to yield silanone, the monomer of the silicone polymers, we have turned our attention to reactions of silylene with O-donors.²⁴ The π -type addition of SiH₂ to Me₂CO represents one of the simplest, if not the prototype, of this class. On the analogy of the SiH₂ + alkene studies the expected initial process is formation of the three-membered ring siloxirane (with C, O, and Si atoms in the ring). Product studies by Ando^{25–27} and others²⁸ have shown that siloxirane rings are formed by such processes and that if protected by large substituents siloxiranes can be sufficiently stabilized for preparative isolation. Ando et al.²⁷ have further shown that the isomeric silacarbonyl ylids are formed in the process preceding siloxirane formation. These ylids are ground-state singlet species of zwitterionic nature. Thus, we anticipate the likely process of reaction here as



The subsequent fate of dimethylsiloxirane and whether it can lead to silanone cannot be determined by the study of the kinetics of SiH₂ removal alone. We have therefore additionally set out to characterize the potential energy surface for this process by ab initio methods. A recent ab initio study²⁹ of the reaction of SiH₂ + H₂CO supports the formation of siloxirane preceded by an ylid complex, which has a significant barrier to siloxirane formation. Gordon and George³⁰ have also calculated

the relative stabilities of a number of isomeric species of formula CSiH_4O that includes the prototype siloxirane ring. There are no previous kinetic or ab initio studies of reaction 1. A preliminary report of our work has appeared.³¹

Experimental Section

Equipment, Chemicals, and Method. The apparatus and equipment for these studies have been described in detail previously.^{32,33} Only essential and brief details are therefore included here. SiH_2 was produced by the 193 nm flash photolysis of phenylsilane (PhSiH_3) using an Oxford Lasers KX2 ArF exciplex laser. Photolysis pulses were fired into a variable temperature quartz reaction vessel with demountable windows, at right angles to its main axis. SiH_2 concentrations were monitored in real time by means of a Coherent 699-21 single-mode dye laser pumped by an Innova 90-5 argon ion laser and operating with rhodamine 6G. The monitoring laser beam was multipassed between 32 and 48 times along the vessel axis, through the reaction zone, to give an effective path length of up to 1.8 m. A portion of the monitoring beam was split before entering the vessel for reference purposes. The monitoring laser was tuned to $17\,259.50\text{ cm}^{-1}$, corresponding to a known strong vibration-rotation transition^{32,34} in the $\text{SiH}_2\text{ A}(^1\text{B}_1) \leftarrow \text{X}(^1\text{A}_1)$ absorption band. Light signals were measured by a dual photodiode/differential amplifier combination, and signal decays were stored in a transient recorder (DataLab DL910) interfaced to a BBC microcomputer. This was used to average the decays of up to 10 photolysis laser shots (at a repetition rate of 1 or 2 Hz). The averaged decay traces were processed by fitting the data to an exponential form using a nonlinear least-squares package. This analysis provided the values for first-order rate coefficients, k_{obs} , for removal of SiH_2 in the presence of known partial pressures of substrate gas.

Gas mixtures for photolysis were made up, containing 1.5–2.5 mTorr of PhSiH_3 and 0–165 mTorr of Me_2CO together with inert diluent (SF_6) at total pressures between 1 and 100 Torr. Pressures were measured by capacitance manometers (MKS, Baratron). Gas chromatographic analysis of product mixtures was carried out using a Perkin-Elmer 8310 chromatograph equipped with a flame ionization detector. Products were separated on a 4 m Porapak Q column operated at 120 °C.

All gases used in this work were thoroughly degassed prior to use. PhSiH_3 (99.9%) was obtained from Ventron-Alfa (Petrarch). Acetone (99+%, Gold Label) was obtained from Aldrich. Sulfur hexafluoride, SF_6 (no GC-detectable impurities), was from Cambrian Gases.

Ab Initio Calculations. The electronic structure calculations were performed with the Gaussian94 software package.³⁵ All structures were determined by energy minimization at the MP2 = Full/6-31G(d) level. Transition-state structures were characterized as first-order saddle points by calculation of the Hessian matrix. Stable structures, corresponding to energy minima, were identified by possessing no negative eigenvalues of the Hessian, while transition states were identified by having one and only one negative eigenvalue. The standard Gaussian-2 (G2) compound method³⁶ was employed to determine final energies for all structures, both for energy minima and transition states. The identities of the transition-state structures were verified by calculation of intrinsic reaction coordinates³⁷ (IRC) at the MP2 = Full/6-31G(d) level. Reaction barriers were calculated as differences in G2 enthalpies at 298.15 K. Additionally, a check was run on the prototype CH_4SiO system at the higher G2Q level³⁸ to test the accuracy of the G2 method on this type of system.

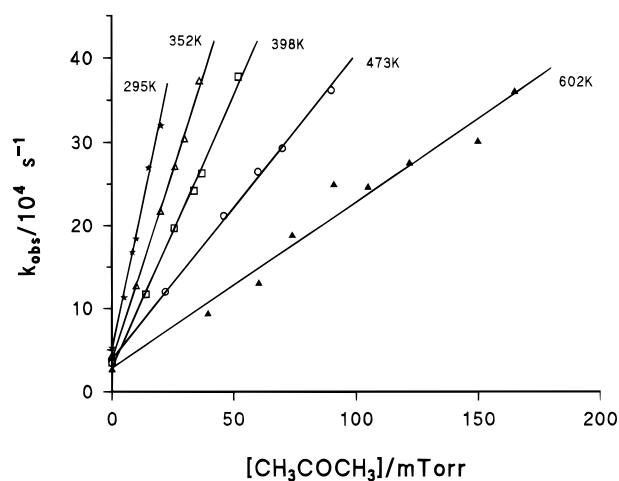


Figure 1. Second-order plots for reaction of SiH_2 with acetone: (*) 295 K, (Δ) 352 K, (\square) 398 K, (\circ) 473 K, (\blacktriangle) 602 K.

TABLE 1: Experimental Second-Order Rate Constants for $\text{SiH}_2 + \text{Me}_2\text{CO}$ at Different Pressures (SF_6)

<i>T</i> /K	$k/10^{-10}\text{ cm}^3\text{ molecule}^{-1}\text{ s}^{-1}$	
	$P_T = 10\text{ Torr}$	$P_T = \infty^a$
295	4.17 ± 0.09	4.2 ± 0.2
352	3.31 ± 0.04	3.3 ± 0.2
398	2.66 ± 0.06	2.6 ± 0.2
473	1.80 ± 0.03	2.0 ± 0.2
602	1.27 ± 0.06	1.7 ± 0.1

^a Obtained by extrapolation; see text.

Results

Kinetics. Preliminary experiments established that, for a given reaction mixture, decomposition decay constants, k_{obs} , were not dependent on the exciplex laser energy (50–80 mJ/pulse, routine variation) or number of photolysis shots (up to 10 shots). The constancy of k_{obs} (five shot averages) showed no effective depletion of reactants. Since acetone is known to absorb 193 nm radiation, tests were carried out that showed that direct decomposition was relatively minor under operating conditions (see Appendix). The sensitivity of detection of SiH_2 was very high but decreased with increasing temperature. Therefore, slightly higher quantities of PhSiH_3 precursor were required at higher temperatures. For the purposes of rate constant measurement at a given temperature PhSiH_3 pressures were kept fixed. A series of experiments were carried out at each of five temperatures in the range 295–602 K. At 10 Torr total pressure (SF_6 diluent), five or six runs (of 5–10 laser shots each) at different Me_2CO pressures were carried out at each temperature. The results of these experiments are shown in Figure 1, which demonstrates the linear dependence of k_{obs} with $[\text{Me}_2\text{CO}]$ expected for second-order kinetics. The second-order rate constants, obtained by least-squares fitting to these plots, are collected in Table 1. The error limits are single standard deviations. It is clear that the rate constants decrease with increasing temperature.

In addition to these experiments, another set of runs was carried out at each temperature in which the total pressure (SF_6) was varied in the range 3–100 Torr in order to test the pressure dependence of the second-order rate constants. In these runs, the second-order plots were obtained with fewer points (two or three substrate pressures provided the fits were good), since the second-order behavior had been established at 10 Torr total pressure. To keep errors to a minimum, sufficient Me_2CO was used to ensure k_{obs} values in the range $(2\text{--}3) \times 10^5\text{ s}^{-1}$ where

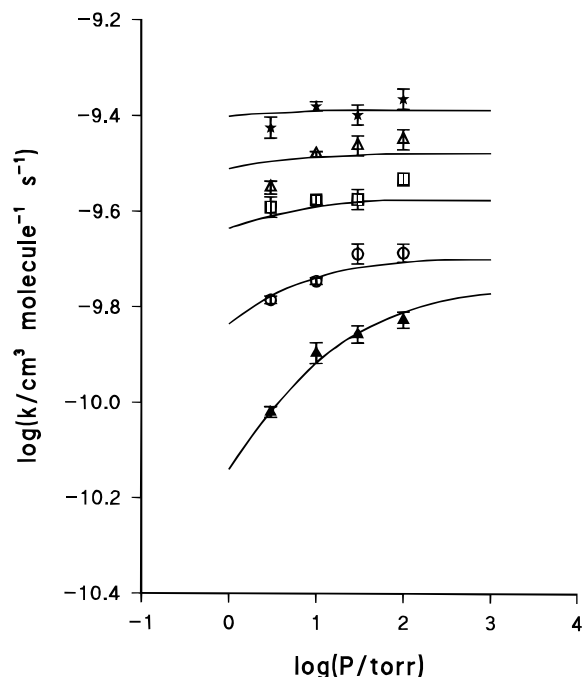


Figure 2. Pressure dependence of second-order rate constants for $\text{SiH}_2 + \text{Me}_2\text{CO}$ at different temperatures: (*) 295 K, (Δ) 352 K, (\square) 398 K, (\circ) 473 K, (\blacktriangle) 602 K. Solid lines are RRKM theoretical fits. P is the total pressure (SF_6).

reaction of SiH_2 with Me_2CO was at least 80% of the total reaction compared with reaction with the precursor. The pressure range was dictated by practical considerations. At pressures above 100 Torr signals were partially quenched, and below 3 Torr pressure measurement uncertainties become significant. The results from these experiments are shown in Figure 2, which shows the pressure dependence of the rate constants at each temperature, in a log–log plot for convenience. The uncertainties (single standard deviations) in individual rate constants are shown in the figure by means of error bars.

It is apparent from Figure 2 that at 295, 352, and 398 K rate constants are effectively constant within experimental error at all pressures. At the higher temperatures of 473 and 602 K rate constants decrease with decreasing pressure, more so at 602 K than at 473 K. High-pressure limiting values of the rate constants, representing the true bimolecular process, are thus easily obtained at the lowest three temperatures, but at the two higher ones they require some extrapolation. These effects are characteristic of a third-body-mediated association reaction, as found in several of our previous studies of SiH_2 reactions,^{8–12,33} and for this reason we have carried out RRKM modeling calculations, described in the next section. These calculations have also been used to assist in the extrapolations, to obtain the values of k^∞ , which are also shown in Table 1. A fit of the data to the Arrhenius equation yielded the following:

$$\log(k^\infty/\text{cm}^3 \text{ molecule}^{-1} \text{ s}^{-1}) = (-10.17 \pm 0.04) + \frac{4.54 \pm 0.32 \text{ kJ mol}^{-1}}{RT \ln 10}$$

The small uncertainties are indicative of a good linear fit (correlation coefficient = 0.992). An Arrhenius plot of the 10 Torr values of k was clearly curved, as found previously for such processes in their pressure-dependent regions.^{8–12}

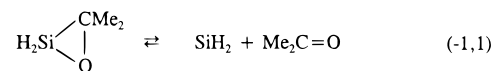
A gas chromatographic search was carried out for reaction products in the room-temperature photolysis studies. Apart from the small amounts of C_1 , C_2 , and C_3 hydrocarbons coming from

TABLE 2: Estimated A Factors for 3,3-Dimethylsiloxirane Decomposition

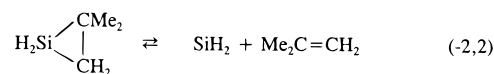
T/K	295	352	398	473	602
$\log(A_1/\text{s}^{-1})$	17.40	17.32	17.25	17.12	16.88

Me_2CO photolysis, the only significant additional product from photolysis of $\text{PhSiH}_3/\text{Me}_2\text{CO}$ mixtures was C_3H_6 , propene.

RRKM Calculations. The pressure dependence of an association reaction corresponds exactly to that of the reverse unimolecular dissociation process provided there are no other perturbing reaction channels. Although we cannot presume that there are no other competing channels, nevertheless as a reference exercise we have carried out RRKM calculations³⁹ of the pressure dependence of the unimolecular decomposition of 3,3-dimethylsiloxirane, i.e.,



Since the dimethylsiloxirane molecule has not yet been isolated and therefore its decomposition kinetics are unknown, we are forced to make estimates of the necessary parameters prior to carrying out calculations. Fortunately, there is a very closely analogous reaction that can be used as a model, viz.,



RRKM calculations on reaction –2 have provided a good fit to the pressure dependence of the kinetics of $\text{SiH}_2 + i\text{-C}_4\text{H}_8$.¹⁰ Thus, we believe that the transition-state structures for these two reactions should be sufficiently similar for us to assume identical entropies of activation and A factors, with the only real difference being in the critical energy, which will reflect the different bonds and strain energies of the two ring systems. The addition kinetics of reaction 2 provides support for this, viz., $A_2/\text{cm}^3 \text{ molecule}^{-1} \text{ s}^{-1} = 10^{-9.91}$ compared to $10^{-10.17}$ for A_1 . The small difference is within the realistic error of the measurements and of the assumptions being made here. The estimated A factors are shown in Table 2. The A_1 values show small but significant variation with T . This arises because of the temperature dependence of ΔS^\ddagger , used in the model reaction –2,2. There is no reason not to assume the same behavior for reaction –1,1. This implies a slight curvature in the Arrhenius plot for the decomposition of 3,3-dimethylsiloxirane over the ca. 300 K temperature range of this study. Although this behavior cannot be independently verified, we believe it reflects the variational character of the transition states for many of the decomposition reactions that result in silylene formation.⁴ There is plenty of indication of this for the decompositions of silirane ring systems.^{8–10}

The next stage was to assign the vibrational wavenumbers of 3,3-dimethylsiloxirane and its activated complex at each temperature of study. This was done first for the molecule itself by taking the harmonic assignment calculated from the ab initio calculations (at the HF/6-31G* level with 11% reduction in the wavenumber values). The activated complex was then assigned by lowering the wavenumbers, principally of the ring modes and SiH_2 group vibrations of the molecule, until a match was obtained with the entropy of activation and the A factor in the usual way.³⁹ Values for other modes were left unchanged except for the C–O stretch wavenumber, which was increased. Methyl group internal rotors were treated as low wavenumber vibrations and left unchanged between molecule and activated complex.

TABLE 3: Molecular and Transition-State Parameters for RRKM Calculations for 3,3-Dimethylsiloxirane Decomposition at 295 K

	3,3-dimethylsiloxirane	3,3-dimethylsiloxirane [‡]
ν/cm^{-1}	2927(2)	2927(2)
	2908(2)	2908(2)
	2854(2)	2854(2)
	2168(2)	2168(2)
	1460(4)	1460(4)
	1396(2)	1396(2)
	1241(1)	1241(1)
	1176(1)	1176(1)
	1121(1)	1121(1)
	989(1)	989(1)
	986(1)	986(1)
	946(1)	946(1)
	926(1)	1700(1)
	875(1)	875(1)
	849(1)	849(1)
	577(1)	577(1)
	357(1)	357(1)
	315(1)	315(1)
	220(1)	220(1)
	213(1)	213(1)
	652(1)	40(2)
	612(1)	33(1)
	531(1)	30(1)
	364(1)	
	773(1)	
reaction coordinate	773 cm^{-1}	
I^{\ddagger}/I	1	
path degeneracy	1	
E_0 (critical energy)	209.6 kJ mol^{-1} (50.1 kcal mol^{-1})	
collision number, $Z_{\text{LJ}}^{a,b}$	$4.56 \times 10^{-10} \text{ cm}^3 \text{ molecule}^{-1} \text{ s}^{-1}$ (SF ₆)	

^a Collision diameters: 3,3-dimethylsiloxirane, 5.40 Å; SF₆, 5.13 Å.

^b LJ temperature (ϵ/k): 3,3-dimethylsiloxirane, 360 K; SF₆, 222 K.

Whether precise values of all vibrational wavenumbers are correct is not important provided the entropy of activation is matched. Because of the apparent decrease in values of the A factor with temperature, we have modified the activated complex wavenumbers at each temperature in order to build in variational character rather than use a temperature-averaged, fixed-wave-number complex. The details are shown in Tables 3 and 4. We have assumed that geometry changes in the decomposing ring molecule do not lead to significant changes in overall moments of inertia and adiabatic rotational effects (angular momentum conservation problems). This is an approximation, in view of the loose activated complex structures, but we believe it will not lead to serious errors. However, we have used a weak collisional (stepladder) model for collisional deactivation,³⁹ since there is considerable evidence against the strong collision assumption.⁴⁰ The average energy removal parameter, $\langle \Delta E \rangle_{\text{down}}$, was taken as 12.0 kJ mol^{-1} (1000 cm^{-1}), similar to that used for silirane.^{8,9} Previously, we have found⁸⁻¹⁰ that variations within the range 8.4–12.0 kJ mol^{-1} had little effect on the fitting.

The critical energy, E_0 , was treated as an adjustable parameter in order not to prejudge the ab initio calculations, there being no experimental source of information on the thermochemistry of 3,3-dimethylsiloxirane or indeed any other siloxirane. Because the pressure dependence is greatest at 602 K (see Figure 2), the test of the quality of fit was carried out at this temperature. Four different values of E_0 were chosen in the range 167–230 kJ mol^{-1} (40–55 kcal mol^{-1}). The results are shown in Figure 3, which clearly demonstrates the sensitivity of the model to changes in E_0 . As can be seen the best fit was obtained with $E_0 = 210 \text{ kJ mol}^{-1}$ (50 kcal mol^{-1}). This value was then used at each temperature of study to obtain a rate constant pressure

TABLE 4: Temperature-Dependent Parameters Used in RRKM Calculations for 3,3-Dimethylsiloxirane Decomposition

T/K	295	352	398	473	602
transition state	40(2)	50(1)	61(1)	70(1)	80(1)
wavenumbers/ cm^{-1}	33(1)	44(1)	50(1)	55(1)	61(1)
	30(1)	40(2)	40(1)	50(1)	60(1)
		30(1)	30(1)	31(1)	40(1)
$E_0/\text{kJ mol}^{-1}$	209.6	209.6	209.6	209.6	209.6
$\Delta H^\circ/\text{kJ mol}^{-1}$	225.4	226.6	227.4	228.5	230.0
$Z_{\text{LJ}}/10^{-10} \text{ cm}^3 \text{ molecule}^{-1} \text{ s}^{-1}$	4.56	4.67	4.75	4.89	5.12

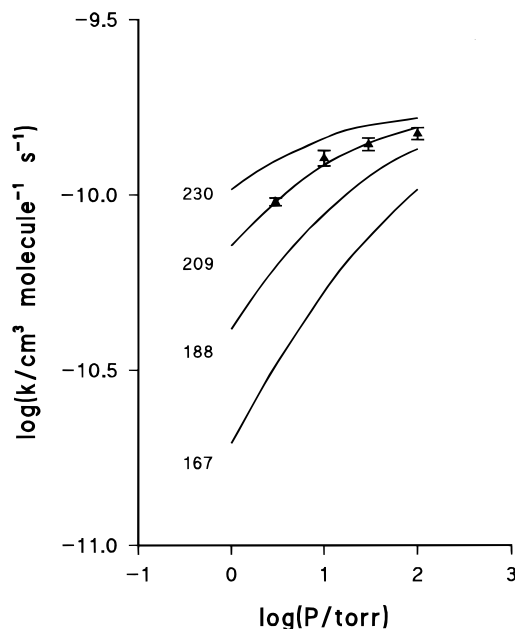


Figure 3. Dependence of RRKM theoretical curves (pressure dependence) on critical energy, $E_0/\text{kJ mol}^{-1}$, for $\text{SiH}_2 + \text{Me}_2\text{CO}$ at 602 K. \blacktriangle indicates experimental data points.

dependence (“fall-off”) curve. The resulting curves are shown in Figure 2 along with the experimental data. The fit to the whole data set is reasonable, bearing in mind that not only are the curvatures significant at 602 and 473 K but also that the curvature is insignificant at other temperatures. The small deviations from the fit of a few data points is probably due to experimental error. For the calculations, no adjustments were made to E_0 at different temperatures for variational character, since this would have been within the error of the calculations. E_0 was converted to E_a by addition of the thermal energy difference between the molecule and its transition state and finally into ΔH° via $\Delta H^\circ = E_a - E_0 + RT$. The resulting values of ΔH° are shown in Table 4.

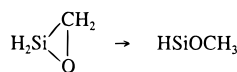
The only problem in this procedure is the extrapolation of the pressure-dependent rate constants (at 473 and 602 K). We have adopted a theoretically assisted procedure for this, as previously.⁸⁻¹² At each temperature an initial approximate (eyeball) estimate of the k^∞ value was obtained to provide the basis for a first attempt at the RRKM calculation for each system. The falloff curves generated were then used to refine k^∞ values to the ones shown in Table 1. Fortunately, the extrapolations were relatively short compared to the range of falloff values, and so this should be quite reliable. The estimated uncertainties in k^∞ values ($\pm 10\%$ or less) are shown in the table. The results of our final calculations are shown as the full curves in Figure 2.

Because of the findings of the ab initio calculations (vide infra), one further set of RRKM calculations was carried out to

investigate the sensitivity of the falloff curves to adjustment of the A factor for the 3,3-dimethylsiloxirane decomposition (i.e., the transition-state structure). TS wavenumbers for the adjustable vibrations were estimated corresponding to $\log(A/s^{-1}) = 16.62$ and 16.36, and new falloff curves were generated at 602 K, with $E_0 = 210 \text{ kJ mol}^{-1}$. When compared with that shown in Figures 2 and 3 ($\log(A/s^{-1}) = 16.88$), the degree of falloff was reduced. The reduction was greater for the lower A factor. The results of these calculations showed that a change of -0.52 in $\log(A/s^{-1})$ corresponded to a change of ca. $+20 \text{ kJ mol}^{-1}$ in E_0 , indicating that a tighter transition state would require a lower value of E_0 to create an equivalent degree of falloff. Given that the model A factor ($\log(A/s^{-1}) = 16.88$ at 602 K) might have been slightly high (by 0.26 in $\log(A/s^{-1})$), this suggests a possible overestimate of E_0 by ca. 10 kJ mol^{-1} , with a likely maximum error of 20 kJ mol^{-1} . ΔH° values in Table 4 could therefore also be overestimated to the same extent.

Ab Initio Calculations. Possible species on the $\text{C}_3\text{H}_8\text{SiO}$ surface were investigated in some detail at the G2 level of theory. Apart from the reactant species, $\text{SiH}_2 + \text{Me}_2\text{CO}$ and the possible products $\text{SiH}_2\text{O} + \text{C}_3\text{H}_6$ (propene), six other energy minima were found together with five transition states. The minima correspond to the silacarbonyl ylid (initial complex of SiH_2 and Me_2CO), 3,3-dimethylsiloxirane, 2-siloxyprene, isopropoxysilylene, 3-methylsiloxetane, and a silanone-propene complex. The transition states linking these species are labeled TS1a, TS1b, and TS2–4. The structures of these species are shown in Figure 4, and their enthalpy values are listed in Table 5, as well as being represented on the potential energy (enthalpy) surface in Figure 5. Among the notable features of the surface (with its mechanistic implications) are (i) the initial formation of a fairly stable silacarbonyl ylid species, (ii) low-energy pathways for rearrangement of the silacarbonyl ylid to (a) a siloxirane ring through ring closure and (b) 2-siloxyprene via a 1,4 H-shift process, (iii) an approximately thermoneutral isomerization process from the siloxirane to alkoxyisilylene, which represents the lowest energy ring-opening pathway for this three-membered ring, and (iv) a high energy C–H insertion reaction step of the silylene to a siloxetane (which can then break down to silanone and propene). As far as energetic considerations alone are concerned, the transition states TS1a, TS1b, and TS2 all lie below threshold, suggesting that, in principle, 3,3-dimethylsiloxirane, 2-siloxyprene, and isopropoxysilylene are all accessible as reaction products. The potential pathway to silanone + propene appears to be blocked by the high-energy barrier associated with TS3.

To test the accuracy of the G2 method used here, a comparison was made at the higher G2Q level of theory for the process,



The overall ΔH° value for this reaction at G2Q was -0.5 kJ mol^{-1} compared with $-13.8 \text{ kJ mol}^{-1}$ at G2. The barrier height at G2Q ($137.6 \text{ kJ mol}^{-1}$) is 10 kJ mol^{-1} higher than that at G2 ($127.7 \text{ kJ mol}^{-1}$). The reverse barrier is therefore only 3 kJ mol^{-1} different at the two levels of theory. This suggests that the energy barrier values found at the G2 level in the main system of this study are probably accurate to within 15 kJ mol^{-1} .

Discussion

General Comments, Comparisons, and the Nature of the Reaction Process. The results reported here represent the first

TABLE 5: Ab Initio (G2) Enthalpies for $\text{C}_3\text{H}_8\text{SiO}$ Species of Interest in the Reaction of Silylene with Acetone

molecular species	energy/hartree	relative energy/ kJ mol^{-1}
$\text{SiH}_2 + \text{Me}_2\text{CO}$	-482.971 144 0	0
$\text{H}_2\text{Si}\cdots\text{OCMe}_2$ complex	-483.002 680 0	-82.8
TS1a	-482.983 267 7	-31.8
3,3-dimethylsiloxirane	-483.042 882 0	-188.3
TS1b	-482.989 421 9	-48.0
2-siloxyprene	-483.066 909 0	-251.4
TS2	-482.995 396 6	-63.7
isopropoxysilylene	-483.043 584 0	-190.2
TS3	-482.967 362 1	+9.9
3-methylsiloxetane	-483.071 264 0	-262.9
TS4	-483.015 463 7	-116.4
$\text{SiH}_2\text{O}\cdots\text{propene}$ complex	-483.030 022 0	-154.6
$\text{SiH}_2\text{O} + \text{propene}$	-483.015 608 0	-116.7

comprehensive investigation of the kinetics of reaction of SiH_2 with acetone, or indeed with any carbonyl-containing species. The growing database of absolute rate constants enables us to compare the reactivity of SiH_2 with several other π -bond-containing species. This is shown in Table 6. The table indicates that both in terms of Arrhenius parameters and absolute rate constants, at 298 K, these reactions have very similar characteristics. The magnitude of the absolute rate constants is close to, if not at, the collision number value, thus showing that these reactions are occurring at every collision (at the true bimolecular limit). The negative activation energies are small and consistent with those expected for normal association reactions.^{10,39,41} Thus, in contrast to the Si–H insertion reaction, for instance that of $\text{SiH}_2 + \text{SiH}_4$,³³ there is no demanding evidence for the involvement of an intermediate complex in any of these reactions. However, the presence of a low-lying bound intermediate with a relatively low barrier to rearrangement is also not ruled out by these results. Indeed, the ab initio calculations (vide infra) point to its existence. For addition reactions of SiMe_2 , as opposed to those of SiH_2 , the larger negative activation energies (e.g., -8.5 kJ mol^{-1} for $\text{SiMe}_2 + \text{C}_2\text{H}_4$ ¹⁰) suggest that intermediates may play a more important role.

Because reaction 1 occurs so rapidly, it is impossible to discern whether the O atom of the carbonyl group plays any special role as an O-donor. However the pressure dependence of this reaction does suggest significant differences in the secondary chemistry of the siloxirane ring, which is illuminated by the ab initio calculations (see next section).

RRKM Calculations, Ab Initio Calculations, and the Reaction Mechanism. For the formation of siloxirane, the RRKM calculations give $\Delta H^\circ = -225 \text{ kJ mol}^{-1}$, possibly overestimated by up to 20 kJ mol^{-1} . The ab initio calculations give $\Delta H^\circ = -188 \text{ kJ mol}^{-1}$, within an expected accuracy of $\pm 15 \text{ kJ mol}^{-1}$. Thus, the experimental results and theoretical calculations are just at the borderline of agreement, assuming that siloxirane ring formation represents the main pathway. The ab initio calculations indicate greater complexity. The initially formed silacarbonyl ylid (intermediate complex) can rearrange to produce 2-siloxyprene via transition state TS1b, which is lower in energy by 16 kJ mol^{-1} than TS1a, the transition state for ring closure to 3,3-dimethylsiloxirane, thus suggesting the possibility of a different pathway. End product studies are ambiguous on this point. Our own search did not reveal a GC peak in the appropriate retention time region. Ando and colleagues^{25–27} and others²⁸ have detected and isolated siloxirane products in reactions of dimethylsilylene with highly substituted ketones and, indeed, in matrix isolation studies²⁷ detected the silacarbonyl ylid intermediates. However, in other studies of SiMe_2 ⁴² and SiPh_2 ⁴³ with simpler carbonyl compounds the

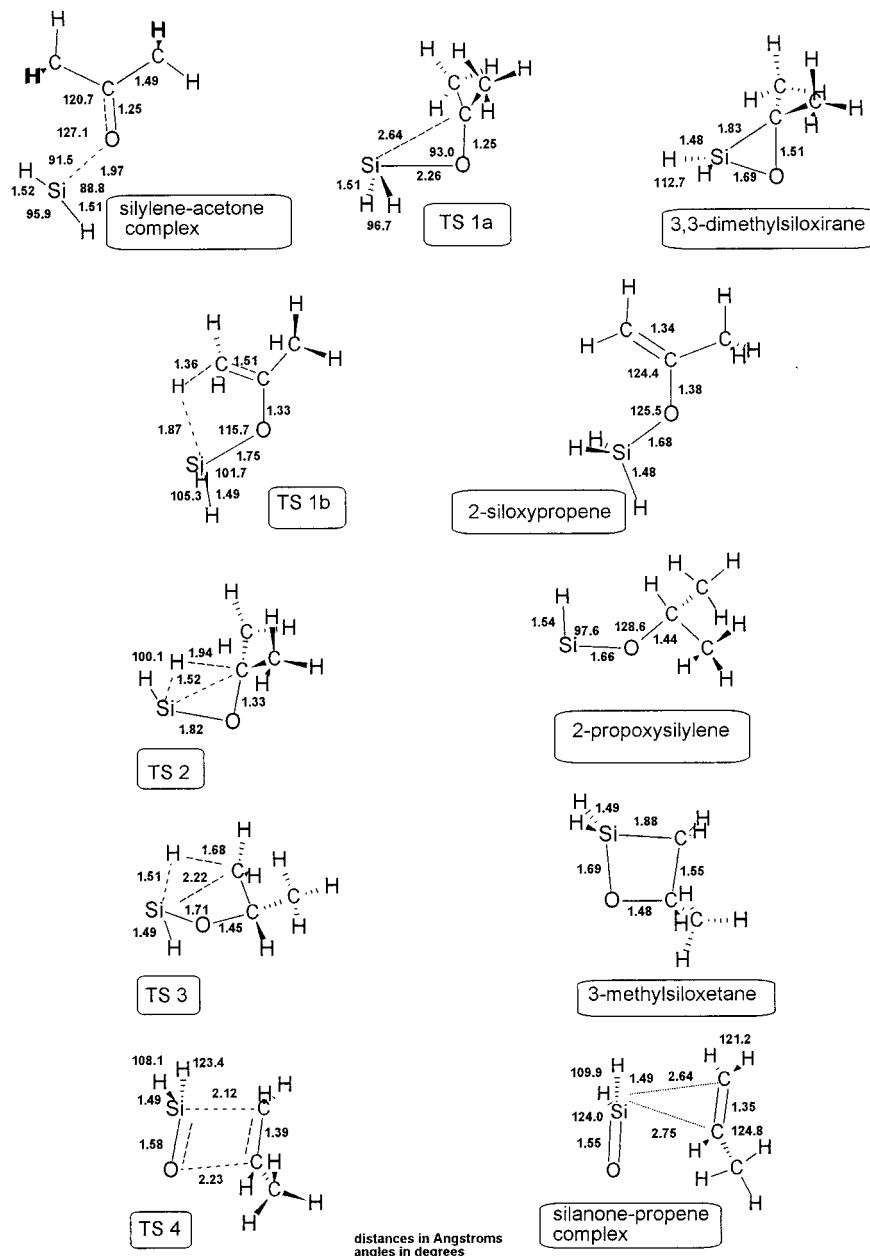


Figure 4. Ab initio MP2 = Full/6-31G(d) calculated geometries of local minimum structures and transition states on the $\text{SiH}_2 + \text{Me}_2\text{O}$ energy surface. Selected distances are given in angstroms and angles in degrees.

products were the silyl enol ethers, corresponding to the alternative pathway. This suggests that these reaction pathways are close in energy and that substituent effects may swing the reaction one way or the other. In the present reaction system, as well as the lack of the appropriate reaction product, there are two further reasons why we doubt that silyl enol ether formation represents the dominant pathway. First, TS1b has a considerably tighter structure than TS1a, i.e., it has a more restrictive entropy requirement, which would offset at least part of the small energy advantage. Second, the observed pressure dependence is not consistent with its formation. A more stable product ($\Delta H^\circ = -251 \text{ kJ mol}^{-1}$) with a tighter transition state than that for the siloxirane formation would be expected to have a much lesser pressure dependence than observed. However, it is possible that a small contribution of this pathway, i.e., as a side reaction, could explain the less than perfect fit of the RRKM calculations to the energetics of siloxirane formation.

While these arguments favor the formation of 3,3-dimethylsiloxirane as the initial product, they do not indicate whether

the siloxirane is capable of further reaction, via TS2, to yield isopropoxysilylene. The ab initio calculations suggest that TS2 is low enough in energy to permit this. They also indicate that the silylene product is slightly more stable than the siloxirane itself. This suggests that isopropoxysilylene may be the ultimate reaction product of reaction in the present study. This contrasts with the reactions of silylene with C_2H_4 and C_2H_2 where the analogous ethyl- and vinylsilylene are accessible from silirane and silirene, respectively, through low-energy transition states, but unstable (thermodynamically) with respect to the rings, so that they revert to them as the stable products as shown via numerous experimental¹²⁻¹⁹ and theoretical²⁰⁻²³ studies. The increased stability of the alkoxy-silylene isomer of a siloxirane is readily accounted for by $p_\pi-p_\pi$ donation from the oxygen lone pair to the empty p orbital of the silylene.⁴ If formed ultimately, the isopropoxysilylene is not seriously affecting the rate-determining addition because TS2 is a tight transition state and overall reaction is occurring at close to the collision rate. Thus, the formation of isopropoxysilylene, if it occurs, is a

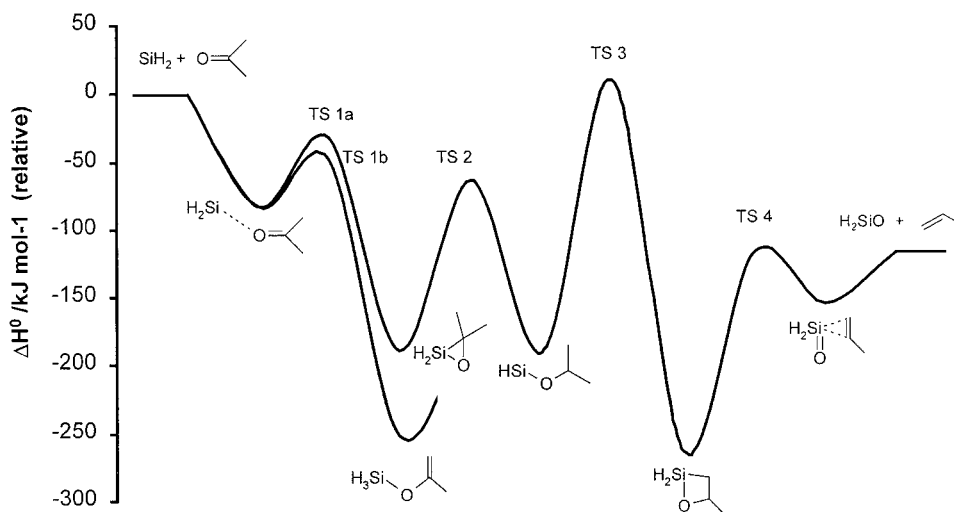


Figure 5. Potential energy (enthalpy) surface for the reaction of $\text{SiH}_2 + \text{Me}_2\text{CO}$. All enthalpies are calculated at the ab initio G2 level.

TABLE 6: Arrhenius Parameters and Room Temperature Rate Constants for Silylene Addition Reactions

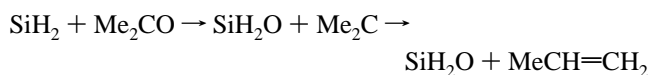
reactants	$\log A^\circ$ ^a	$E_a/\text{kJ mol}^{-1}$	$k^\infty(298\text{ K})^\circ$	ref
$\text{SiH}_2 + \text{C}_2\text{H}_2$	-9.99 ± 0.03	-3.3 ± 0.2	4.0×10^{-10}	12
$\text{SiH}_2 + \text{C}_2\text{H}_4$	-9.97 ± 0.03	-2.9 ± 0.2	3.5×10^{-10}	9
$\text{SiH}_2 + \text{C}_3\text{H}_6$	-9.79 ± 0.05	-1.9 ± 0.3	3.4×10^{-10}	10
$\text{SiH}_2 + i\text{-C}_4\text{H}_8$	-9.91 ± 0.04	-2.45 ± 0.3	3.2×10^{-10}	10
$\text{SiH}_2 + \text{Me}_2\text{CO}$	-10.17 ± 0.04	-4.5 ± 0.3	4.2×10^{-10}	this work

^a Units: $\text{cm}^3 \text{ molecule}^{-1} \text{ s}^{-1}$.

secondary process arising from vibrationally excited 3,3-dimethylsiloxirane molecules formed, chemically activated, from the initial addition reaction. To test for this part of the mechanism, we are currently undertaking appropriate isotopic labeling experiments on the analogous $\text{SiH}_2 + \text{acetaldehyde}$ reaction system⁴⁴ to find out whether scrambling can occur via reversible formation of the isomeric silylene, a mechanism similar to that found in silylene addition to alkenes and alkynes.^{4,5,12,13}

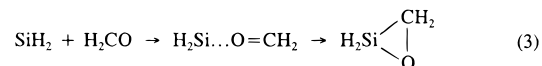
The remaining part of the potential surface presented here was obtained with a view to trying to see whether an obvious route existed for the formation of propene (plus silanone). Our finding is that the pathway via 3-methylsiloxetane is too high in energy (TS3) to make it a likely candidate for subsequent propene formation even though the siloxetane if formed would have sufficient energy to break down to propene and silanone via TS4 and the weakly bound propene/silanone complex. Even allowing for uncertainties in our calculated transition-state energies, this conclusion is likely to stand up because TS3 has the added handicap of being a tight transition state, making it also restricted on entropy grounds. The difficulty of the intramolecular 1,4 C–H insertion by isopropoxysilylene again probably arises from the stabilizing effect of the alkoxy substituent in the silylene. There is some debate over whether a 1,4 C–H insertion can occur in an alkylsilylene such as *n*-propyl silylene,⁴⁵ although it is known that the reverse process of intramolecular silylene extrusion from a siletane is competitive with siletane cleavage⁴⁶ (i.e., when oxygen is not present in the ring).

The only other plausible route (not shown in the diagram) is the direct abstraction pathway, leading in the initial stage to dimethylcarbene, viz.,



An ab initio check on the dimethylcarbene (S_1 state)/propene enthalpy difference at the G2 level gives a value of 281 kJ mol^{-1} . This means that the first stage of this process is significantly endothermic (by ca. 164 kJ mol^{-1}), which rules out this mechanism as a pathway to propene formation. Thus, we are unable to offer a plausible direct route to the propene product found experimentally. It is possible that it could have arisen by photolysis of one of the other silicon-containing species initially formed in this system.

During the course of this study a theoretical calculation by Lu et al.²⁹ on the potential energy surface of the reaction of $\text{SiH}_2 + \text{H}_2\text{CO}$ suggested the analogous mechanism, viz.,



At the MP2/6-31G**//6-31G* level the ylid intermediate was found to be 37.8 kJ mol^{-1} below the reactants but the transition state for closure to the siloxirane ring was 13.6 kJ mol^{-1} above the reactants. We plan to investigate this surface ourselves, since it implies that reaction 3 should have a positive overall activation energy, which seems unlikely from the results of the present study taken together with our earlier findings on the kinetics of SiH_2 addition reactions.^{8–12}

Apart from this the only other related calculations are those of Gordon and George³⁰ who calculated the energies of siloxirane and some of its isomers. The species in these calculations, apart from the siloxirane ring itself, were not counterparts of those of the present study.

Acknowledgment. R.B. and R.W. thank Dow-Corning for a grant in support of the experimental work. R.B. also thanks the Spanish DG1CYT (PB97-1214). J.P.C. thanks Dr. Carlos Sosa (SGI-Cray Research) for help and advice with the theoretical calculations. We also thank a referee for raising issues concerning direct acetone photodecomposition (see below).

Appendix: Effect of Direct Photodecomposition of Acetone

Acetone has an absorption coefficient at 193 nm of ca. $3.8 \times 10^{-18} \text{ cm}^2$ ⁴⁷ and is known to decompose to produce two methyl radicals and CO with a quantum efficiency of ca. 0.96.⁴⁸ Under the operating conditions in this study, with a 4 cm^2 beam cross section and a typical pulse energy of 60 mJ, this leads to ca. 6% decomposition of acetone. At the low substrate pressures

TABLE 7: Dependence of SiH₂ Signal Decay Constant on Excimer Laser Pulse Energy

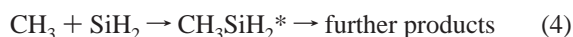
series 1 ^a		series 2 ^b	
energy/mJ ^c	<i>k</i> _{obs} /10 ⁴ s ^{-1 d}	energy/mJ ^c	<i>k</i> _{obs} /10 ⁴ s ^{-1 d}
20	32.6	40	18.4
50	31.9	65	18.5
75	32.8	85	20.8
110	31.0	100	20.1
130	32.0	130	19.5

^a *T* = 295 K; PhSiH₃ (1.7 mTorr), Me₂CO (22 mTorr), SF₆ (10 Torr).

^b *T* = 473 K; PhSiH₃ (1.7 mTorr), Me₂CO (50 mTorr), SF₆ (10 Torr).

^c Pulse energies measured at laser output coupler. Losses from steering optics and cell wall entry area probably amount to ca. 30%. ^d Uncertainties of fitting ca. 5–10%.

(mTorr), with a path length of 4 cm (reaction vessel diameter; lateral beam entry) the system is optically thin and the methyl radicals should be produced uniformly within the cell. GC analysis confirmed the formation of typical radical products, CH₄ and C₂H₆ (as well as the cited C₃H₆). The question arises as to whether the reaction system can be perturbed by reaction of CH₃ with SiH₂, viz.,



Chromatograms show no significant peaks suggestive of any new product, although several small peaks were present, apart from CH₄, C₂H₄, and C₃H₆, at ca. 5% of the C₂H₆ yield.

Since the methyl radical yield is dependent on the excimer laser pulse energy, we decided to carry out a test to vary the pulse energy as widely as possible to look for any effect on the SiH₂ decay characteristics under typical experimental conditions. Two sets of experiments were carried out, using typical reaction mixtures at 295 and 473 K, with variation of the laser pulse energy between 20 and 130 mJ. SiH₂ traces were found to give excellent exponential fits up to 90% decay in all cases (five shot averages) and to be repeatable. The results are shown in Table 7. It is apparent from the table that over a range of a factor of 6.5 variation in photolysis laser intensity at ambient temperatures and 3.2 at 473 K, the decay traces show no variation of rate constant outside of reasonable experimental error. This indicates strongly to us that, at most, reaction 4 is a small perturbation on the target SiH₂ + Me₂CO reaction. Since the latter is occurring at close to the collision rate, it is unlikely that the perturbing reaction could contribute more than 10% to the overall [SiH₂] decay process, and this would be on the assumption of equal rate constants for reactions 1 and 4. A lower contribution is more likely. The general overall uncertainty in the measured rate constants (systematic as well as random errors) is estimated at ca. ±10%. Thus, the potential perturbing effect of reaction 4 on the measurements reported here can be safely neglected.

References and Notes

- Gaspar, P. P. In *Reactive Intermediates*; Jones, M. Jr., Moss, R. A., Eds.; Wiley: New York, 1978 (Vol. 1, p 229), 1981 (Vol. 2, p 335), 1985 (Vol. 3, p 333).
- Tang, Y. N. In *Reactive Intermediates*; Abramovitch, R. A., Ed.; Plenum: New York, 1982; Vol. 2, p 297.
- Safarik, I.; Sandhu, V.; Lown, E. M.; Strausz, O. P.; Bell, T. N. *Res. Chem. Intermed.* **1990**, *14*, 105.
- Becerra, R.; Walsh, R. In *Research in Chemical Kinetics*; Compton, R. G., Hancock, G. M., Eds; Elsevier: Amsterdam, 1995; Vol. 3, p 263.
- Jasinski, J. M.; Becerra, R.; Walsh, R. *Chem. Res.* **1995**, *95*, 1203.
- Apeloig, Y. In *The Chemistry of Organic Silicon Compounds*; Patai, S., Rappoport, Z., Eds; Wiley: New York, 1989; Vol. 1, p 57.
- Gordon, M. S.; Francisco, J. S.; Schlegel, H. B. *Adv. Silicon Chem.* **1993**, *2*, 137.

- Al-Rubaiey, N.; Frey, H. M.; Mason, B. P.; McMahon, C.; Walsh, R. *Chem. Phys. Lett.* **1993**, *204*, 301.
- Al-Rubaiey, N.; Walsh, R. *J. Phys. Chem.* **1994**, *98*, 5303.
- Al-Rubaiey, N.; Carpenter, I. W.; Walsh, R.; Becerra, R.; Gordon, M. S. *J. Phys. Chem. A* **1998**, *102*, 8564.
- Becerra, R.; Frey, H. M.; Mason, B. P.; Walsh, R. *J. Chem. Soc., Chem. Commun.* **1993**, 1050.
- Becerra, R.; Walsh, R. *Int. J. Chem. Kinet.* **1994**, *26*, 45.
- Al-Rubaiey, N.; Walsh, R. Unpublished results.
- Barton, T. J.; Burns, S. A.; Burns, G. T. *Organometallics* **1983**, *2*, 199.
- Barton, T. J.; Burns, G. T. *Tetrahedron Lett.* **1983**, *24*, 159.
- Rickborn, S. F.; Ring, M. A.; O'Neal, H. E.; Coffey, D., Jr. *Int. J. Chem. Kinet.* **1984**, *16*, 289.
- Erwin, J. W.; Ring, M. A.; O'Neal, H. E. *Int. J. Chem. Kinet.* **1985**, *17*, 1067.
- Rogers, D. S.; O'Neal, H. E.; Ring, M. A. *Organometallics* **1986**, *5*, 1467.
- Rogers, D. S.; Ring, M. A.; O'Neal, H. E. *Organometallics* **1986**, *5*, 1521.
- Nguyen, M. T.; Sengupta, D.; Vanquickenborne, L. G. *Chem. Phys. Lett.* **1995**, *240*, 513.
- Sengupta, D.; Nguyen, M. T. *Mol. Phys.* **89**, 1567.
- Skandke, P. N.; Hrovat, D. A.; Borden, W. T. *J. Am. Chem. Soc.* **1997**, *119*, 8012.
- Skandke, P. N.; Hrovat, D. A.; Borden, W. T. In press.
- For earlier kinetic studies of silylenes (SiH₂ and SiMe₂) with O-donors see review articles in refs 4 and 5 and references therein.
- Ando, W.; Ikeno, M.; Sekiguchi, A. *J. Am. Chem. Soc.* **1977**, *99*, 6447.
- Ando, W.; Hamada, Y.; Sekiguchi, A. *Tetrahedron Lett.* **1982**, *23*, 5323.
- Ando, W.; Hagiwara, K.; Sekiguchi, A. *Organometallics* **1987**, *6*, 2270.
- Beltzner, J.; Ihmels, H.; Pauletto, L.; Noltemeyer, M. *J. Org. Chem.* **1996**, *61*, 3315.
- Lu, X.-H.; Wang, Y.-X.; Liu, C.-B.; Deng, C.-H. *Acta Chim. Sin.* **1998**, *56*, 1075.
- Gordon, M. S.; George, C. *J. Am. Chem. Soc.* **1984**, *106*, 609.
- Becerra, R.; Cannady, J. P.; Walsh, R. XIth International Symposium on Organosilicon Chemistry, Montpellier, France, Sept 1–6, 1996; Paper PC75.
- Baggott, J. E.; Frey, H. M.; King, K. D.; Lightfoot, P. D.; Walsh, R.; Watts, I. M. *J. Phys. Chem.* **1988**, *92*, 4025.
- Becerra, R.; Frey, H. M.; Mason, B. P.; Walsh, R.; Gordon, M. S. *J. Chem. Soc., Faraday Trans.* **1995**, *91*, 2723.
- Jasinski, J. M.; Chu, J. O. *J. Chem. Phys.* **1988**, *88*, 1678.
- Frisch, M. J.; Trucks, G. W.; Schlegel, H. B.; Gill, P. M. W.; Johnson, B. G.; Robb, M. A.; Cheeseman, J. R.; Keith, T.; Petersson, G. A.; Montgomery, J. A.; Raghavachari, K.; Al-Laham, M. A.; Zakrzewski, V. G.; Ortiz, J. V.; Foresman, J. B.; Cioslowski, J.; Stefanov, B. B.; Nanayakkara, A.; Challacombe, M.; Peng, C. Y.; Ayala, P. Y.; Chen, W.; Wong, M. W.; Andres, J. L.; Replogle, E. S.; Gomperts, R.; Martin, R. L.; Fox, D. J.; Binkley, J. S.; Defrees, D. J.; Baker, J.; Stewart, J. P.; Head-Gordon, M.; Gonzales, C.; Pople, J. A. *Gaussian 94*, revision E.2; Gaussian Inc.: Pittsburgh, PA, 1995.
- Curtiss, L. A.; Raghavachari, K.; Trucks, G. W.; Pople, J. A. *J. Chem. Phys.* **1991**, *94*, 7221.
- Gonzales, C.; Schlegel, H. B. *J. Chem. Phys.* **1989**, *90*, 2154.
- Durant, J. L.; Rohlfing, C. M. *J. Chem. Phys.* **1993**, *98*, 8031.
- Holbrook, K. A.; Pilling, M. J.; Robertson, S. H. *Unimolecular Reactions*, 2nd ed.; Wiley: Chichester, 1996.
- Heymann, M.; Hippler, H.; Troe, J. *J. Chem. Phys.* **1984**, *80*, 1853.
- Davies, J. W.; Pilling, M. J. In *Bimolecular Collisions*; Ashfold, M. N. R., Baggott, J. E., Eds.; Advances in Gas Phase Photochemistry; Royal Society of Chemistry: London, 1989; Chapter 3, p 105.
- Ando, W.; Ikeno, M. *Chem. Lett.* **1978**, 609.
- Bobbitt, K. L.; Gaspar, P. P. *J. Organomet. Chem.* **1995**, *499*, 17.
- Becerra, R.; Cannady, J. P.; Walsh, R. Investigations in progress.
- Sawrey, B. A.; O'Neal, H. E.; Ring, M. A.; Coffey, D., Jr. *Int. J. Chem. Kinet.* **1984**, *16*, 801.
- Davidson, I. M. T.; Fenton, A.; Ijadi-Maghsoodhi, S.; Scampton, R. J.; Auner, N.; Grobe, J.; Tillman, N.; Barton, T. *J. Organometallics* **1984**, *3*, 1593.
- Woodbridge, E. L.; Fletcher, T. R.; Leone, S. R. *J. Phys. Chem.* **1988**, *92*, 5387.
- Brouard, M.; MacPherson, M. T.; Pilling, M. J.; Tulloch, J. M.; Williamson, A. P. *Chem. Phys. Lett.* **1985**, *113*, 413.